HTML ABSTRACT • LINKS

Piezoresistance of carbon nanotubes on deformable thin-film membranes

Randal J. Grow, Qian Wang, Jien Cao, Dunwei Wang, and Hongjie Dai[a)]
Department of Chemistry, Stanford University, Stanford, California 94305

(Received 8 September 2004; accepted 10 January 2005; published online 23 February 2005)

Carbon nanotubes have interesting electromechanical properties that may enable a new class of nanoscale mechanical sensors. We fabricated two-terminal nanotube devices on silicon nitride membranes, measured their electronic transport versus strain, and estimated their band gaps and the strain-induced changes in them. We found band-gap increases and decreases among both semiconducting and small-gap semiconducting (SGS) tubes. The SGS band gaps exceeded the predicted curvature-induced gaps for their diameter. Some of the band-gap changes for both types of tubes exceeded the predicted maxima. These anomalies are likely caused by interaction with the rough silicon nitride surface. © *2005 American Institute of Physics*. [DOI: 10.1063/1.1872221]

Carbon nanotubes have attracted much interest in recent years because of their unique electronic and mechanical properties.[1–3] Electronically, they can be metallic, semiconducting, or small-gap semiconducting (SGS), depending on the orientation of the graphene lattice with respect to the axis of the tube. Their electromechanical properties are also interesting[4] and could lead to their use as piezoresistors in mechanical sensors such as strain gauges, pressure sensors, and accelerometers. Theorists have modeled nanotubes under axial strain and torsion and have predicted chirality-dependent band-gap changes up to ~100 meV/% strain.[5–9] In an early experiment, Tombler *et al.*[10] used an atomic force microscope (AFM) tip to stretch a metallic nanotube suspended across a trench. They found a two-order-of-magnitude conductance decrease and explained it by local deformation of the tube at the tip-tube contact. Others suggested that for an SGS tube, axial strain could induce a band-gap increase.[11] Cao *et al.*[12] stretched tubes suspended between a micromachined cantilever and platform and observed conductance decreases in all three types. Minot *et al.*[13] used a method similar to Tombler's to measure suspended tubes, estimated their band gaps (E_g) and rates of change with strain ($dE_g/d\varepsilon$), and found them to agree with theory.

Here we present measurements of the electromechanical response of nanotubes adhering to surfaces. We made devices consisting of metal-contacted tubes on silicon nitride membranes (Fig. 1) similar to those used in micromachined pressure sensors.[14] The tubes adhere to the surface by van der Waals forces and are also held down by the electrodes, so they experience the same strain as the membrane when it is deformed.

First, we used low-pressure chemical vapor deposition to put 1.14 μm of low-stress silicon nitride on 4 in. wafers of (100) silicon. We opened a pattern on the backside and used KOH to etch the silicon anisotropically through the wafer to define 1035 μm^2 nitride membranes. We then grew single-walled nanotubes from patterned catalyst islands and evaporated Pd electrodes to contact them.[15–18] The device gaps were 0.3–1.0 μm. Finally, we evaporated 15–20 nm of Ti/Pd onto the back of the membrane to form a common gate electrode.

[a)]Author to whom correspondence should be addressed; electronic mail: hdai1@stanford.edu

Using finite element analysis, we calculated the strain distribution on the membrane from the measured side length of 1035±5 μm, a thickness of 1.15±0.05 μm, and material properties typical of the silicon nitride produced by our deposition system (residual stress=90±10 MPa, Young's modulus=255±25 GPa, Poisson's ratio=0.263). We varied the pressure from 0 to 20 psi, which gave us the strains in both x and y, which range up to 0.2% on the membrane. The uncertainties in the inputs result in ±8% uncertainty in the strain.

We confirmed with AFM that the devices were single tubes and measured their diameter and their angle with the electrodes, which allowed us to calculate the net strain along the tube from the x and y components of the strain at that point. To avoid water vapor and oxygen effects, we bathed our devices in argon or nitrogen. We applied pressure to the membrane with a standard gas regulator and measured it with a separate diaphragm pressure gauge with resolution of <1 psi.

We measured current versus gate voltage ($I_{ds}-V_g$) for twelve single-tube devices on three different chips under a 10 mV bias (V_{ds}). We found eight SGS, four semiconducting, and no truly metallic tubes with no gate dependence. The on-state resistances were 7–25 kΩ, close to the quantum resistance of 6.5 kΩ, due to the high transparency of the Pd contacts.[17,18] While varying the pressure from 0 to 15 psi in 1 and 5 psi increments, we measured $I_{ds}-V_g$ [Figs. 2(a)–2(c)] and current versus time ($I_{ds}-t$) (Fig. 3). Figure 2(a) shows $I_{ds}-V_g$ curves for one device. The dip is typical

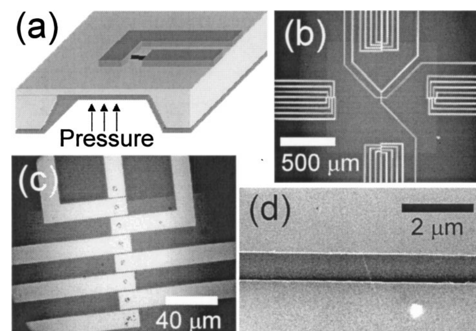

FIG. 1. (a) Schematic of a nanotube device on a membrane. The bottom layer is the gate electrode. (b) Optical microscope image of a membrane (~1 mm on a side) with electrodes. (c) Zoomed-in image of devices (14 μm apart) near the edge of the membrane. (d) SEM image of a nanotube crossing the gap (~800 nm) between two electrodes.

 © 2005 American Institute of Physics
Downloaded 24 Feb 2005 to 171.64.120.244. Redistribution subject to AIP license or copyright, see http://apl.aip.org/apl/copyright.jsp

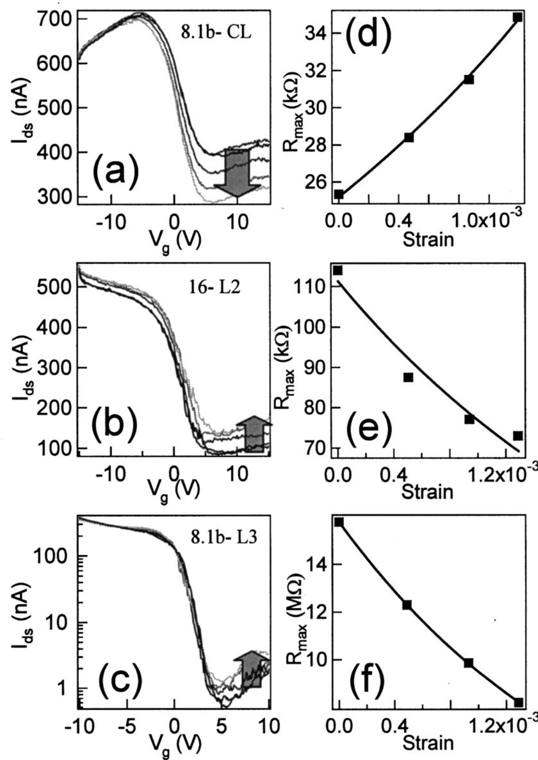

FIG. 2. (a)–(c) I_{ds}-V_g curves for nanotube devices on the membrane at 0, 5, 10, 15, and 0 psi (V_{ds}=10 mV). The arrows show which way the curves moved as the pressure increased. (d)–(f) R_{max} values of the I_{ds}-V_g curves vs simulated strain and a fit to an exponential.

of an SGS tube,[19,20] and the conductance decreased with increasing pressure. The second 0 psi curve, taken after the pressure changes, overlaps the first one, ruling out significant drift or hysteresis. Figure 2(b) shows curves for another SGS device with increasing conductance, and Fig. 2(c) shows them for a semiconducting tube, characterized by a three-order-of-magnitude change from the on to the off state,[21] also with increasing conductance. Figure 3 shows $I_{ds}-t$ for the same device as Fig. 2(b) with the pressure alternately increased in 1 psi increments and returned to zero. We estimate the sensitivity of the device as a pressure sensor as 1 psi. Four of the SGS tubes showed conductance increases and four showed decreases. Three of the semiconducting tubes showed increases and one showed a decrease.

We attribute these changes to changes in the band gap of the nanotube rather than to changes in the contacts because the off current is much more sensitive than the on current. We can estimate E_g and $dE_g/d\varepsilon$ for our tubes by calculating R_{max} from the minima of the $I_{ds}-V_g$ curves, plotting it versus simulated strain, and fitting to it a curve of the form $R_{max}(\varepsilon)=R_0+R_1\exp(\beta\varepsilon)$ [Figs. 2(d)–2(f)]. In the off state, assuming the absence of tunneling through the Schottky barriers at the contacts (since the barrier width is large due to the thick gate dielectric), the resistance is[13]

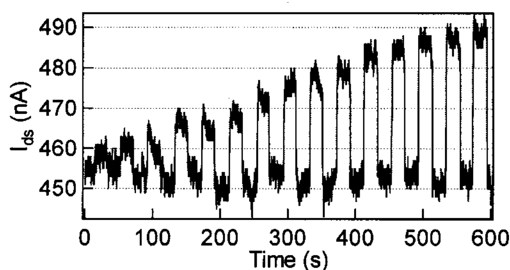

FIG. 3. I_{ds}-t curves from 0 to 15 psi for the SGS device in Fig. 2(b) (V_{ds} =10 mV, gate grounded). The pressure was alternated between zero and a positive pressure increasing in 1 psi increments.

TABLE I. Summary of band-gap information, AFM-measured tube diameter, and gauge factor for ten devices.

Device	Type	E_g (meV)	$dE_g/d\varepsilon$ (meV/%)	d (nm)	Gauge factor
8.1a-CT	SGS	19.7±0.3	−13.9±3.3	1.8±0.8	−35
8.1a-CR	SGS	44.4±0.1	−68.7±1.0	5.6±0.8	−121
8.1b-CL	SGS	24.8±0.3	91.5±2.9	2.5±0.8	315
8.1b-B4	SGS	40.5±0.6	180.9±6.9	3.4±0.8	856
8.1b-L3	Semi.	186.0±0.1	−132.2±0.5	4.4±0.8	−376
8.1b-R2	Semi.	173.0±0.6	−106.7±9.4	3.7±0.8	−317
8.1b-R3	SGS	61.9±0.5	49.5±6.2	3.1±0.8	206
16-T1	SGS	28.2±0.4	−30.0±5.4	2.6±0.8	−81
16-B4	SGS	42.9±0.1	12.1±1.2	3.0±0.8	40
16-L2	SGS	64.1±1.1	−102.5±15.8	2.3±0.8	−300

$$R_{max}=R_S+\frac{1}{|t|^2}\frac{h}{8e^2}\left(1+\exp\left(\frac{E_g}{kT}\right)\right), \quad (1)$$

where R_S is a series resistance and $|t|^2$ is the transmission through the tube. The fitting parameters correspond to

$$R_0=R_S+\frac{h}{|t|^2 8e^2},\quad R_1=\frac{h}{|t|^2 8e^2}\exp\left(\frac{E_g^0}{kT}\right),\text{ and }\beta=\frac{1}{kT}\frac{dE_g}{d\varepsilon}. \quad (2)$$

R_S is negligible because the Pd contacts are transparent, and $|t|^2=6.5\ k\Omega/R_{on}$. From the fit parameters and Eqs. (2), we calculate values for E_g and $dE_g/d\varepsilon$ for the ten of our devices for which there was enough data (Table I).

For semiconducting and metallic tubes, E_g and its strain dependence are predicted by[1,8]

$$E_g=\frac{2\gamma a}{\sqrt{3}d}+\text{sgn}(2p+1)3\gamma[(1+\nu)\varepsilon\cos 3\alpha+\xi\sin 3\alpha], \quad (3)$$

where γ is the tight-binding overlap integral (~2.6 eV),[22] a is the graphene lattice unit vector length (~2.49 Å), and d is the tube diameter. In the second term, p is defined by the nanotube indices $n-m=3q+p$, ν is Poisson's ratio (~0.20), α is the chiral angle, ε is the axial strain, and ξ is the torsion. Intrinsic SGS tubes are those for which $n-m=3q$, and their band gap arises from the curvature of the graphene sheet alone. The band gap and its strain sensitivity are given by[9]

$$E_g=\left|\left(\frac{\gamma a^2}{4d^2}-\frac{ab\sqrt{3}}{2}\varepsilon\right)\cos 3\alpha-\frac{ab\sqrt{3}}{2}\xi\sin 3\alpha\right|, \quad (4)$$

where b is the rate of change of the transfer integral with change in the bond length (~3.5 eV/Å).

Equations (3) and (4) relate the unstrained band gaps of tubes to their diameter. We plot our devices in Fig. 4. The semiconducting band gaps are close to the theory, but the SGS band gaps are larger than expected (<20 meV) and show no correlation to diameter.

Mechanisms other than strain and torsion affect the band gaps of tubes. Transverse collapse of tubes can induce a band gap of up to 0.1 eV in metallic or SGS tubes.[23] The van der

Downloaded 24 Feb 2005 to 171.64.120.244. Redistribution subject to AIP license or copyright, see http://apl.aip.org/apl/copyright.jsp

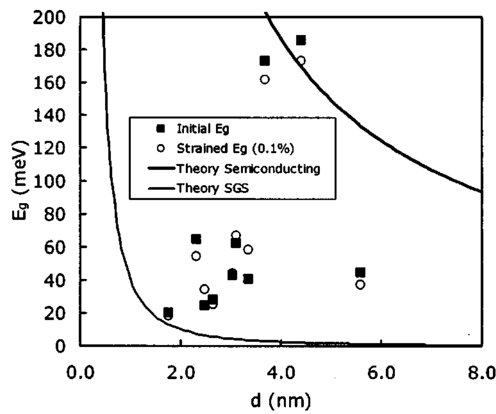

FIG. 4. E_g at 0 and 0.1% strain vs tube diameter for ten devices along with theory curves.

Waals interaction between a tube and a smooth surface can partially collapse it.[24] In addition, if tubes form covalent bonds with silicon nitride, as they have recently been predicted to do with some metals,[25] this could change the band gap directly by changing the electronic structure or indirectly by deforming the tube. The roughness of the silicon nitride (1 nm rms) likely induces local strains, torsions, and collapses along the tube even when the membrane is unstrained. Our "SGS" tubes are likely metallic or intrinsic SGS tubes (curvature-induced band gap) with band gaps increased by these effects, which may also explain why none of the tubes behaved as metallic. In multiwalled tubes, interaction between shells can open a band gap of ~50 meV in a metallic tube or even more in an SGS tube.[26] In bundles, interaction between tubes can induce a band gap in metallic tubes.[27] Some of the larger-diameter tubes may actually be multiwalled or bundles.

According to Eqs. (3) and (4), small axial strains ($<0.2\%$) can induce band-gap increases or decreases in semiconducting tubes, but only decreases in intrinsic SGS tubes, and no change in metallic tubes. We found increases and decreases for semiconducting and "SGS" tubes. In addition, some of the measured $dE_g/d\varepsilon$ values exceed the predicted maxima of ± 94 meV/% for semiconducting and -75 meV/% for SGS, and this cannot be accounted for by the uncertainty in the strain. Surface interactions probably translate increased strain in the membrane into a combination of axial strain, torsion, and collapse in the tube, which change band gaps differently than axial strain alone would. For example, metallic or SGS tubes have band-gap increases under torsion or collapse, which could explain the observed band-gap increases in the "SGS" tubes. In addition, adding torsion and collapse to axial strain could account for the anomalously large responses of some of the tubes.

In conclusion, we have measured the electromechanical response of carbon nanotubes on silicon nitride membranes. Semiconducting and "SGS" tubes both showed both increases and decreases in conductance, probably because the rough substrate caused some of the tubes to experience torsion and collapse in addition to axial strain. The deformation also appeared to increase the unstrained band gaps of the "SGS" tubes, some of which may have been intrinsically metallic. In addition, some tubes showed anomalously large responses, probably also caused by interaction with the surface. Clearly, interaction with a rough substrate strongly affects both the band gaps and the electromechanical responses of the tubes. This may be an area for additional theoretical exploration.

In order to compare nanotubes with silicon piezoresistors, we have calculated the gauge factor $\beta_{\mathrm{GF}}=(\Delta R/R)/\varepsilon$ from the $I_{\mathrm{ds}}-V_g$ curves (Table I). In the off state, where they are most sensitive, the semiconducting and "SGS" tubes have gauge factors of up to 400 and 850, respectively. The maximum achievable in silicon is 200.[28] In addition, nanotubes have a much lower thermal coefficient of resistivity due to the reduced phase space for phonon scattering in a one-dimensional system.[29] In ballistic devices, the temperature dependence can even disappear.[18] Nanotubes could also be utilized on a variety of substrates, including flexible plastics.

One of the authors (R. J. G.) acknowledges the support of the NDSEG Fellowship. The work was also supported by NSF-NIRT. We did the silicon fabrication in the Stanford Nanofabrication Facility, supported by NSF. We would like to thank SNF REU students John Liu and Robert Caldwell for help with initial fabrication, Baris Bayram for help with ANSYS, and Ali Javey, David Mann, Marco Rolandi, Tom Kenny, and Cal Quate for useful discussions.

[1] M. S. Dresselhaus, G. Dresselhaus, and P. C. Eklund, *Science of Fullerenes and Carbon Nanotubes* (Academic, San Diego, 1996).
[2] M. S. Dresselhaus, G. Dresselhaus, and P. Avouris, *Carbon Nanotubes: Synthesis, Structure, Properties, and Applications* (Springer, Berlin, 2001), Vol. 80.
[3] H. Dai, Surf. Sci. **500**, 218 (2002).
[4] A. Maiti, Nat. Mater. **2**, 440 (2003).
[5] C. L. Kane and E. J. Mele, Phys. Rev. Lett. **78**, 1932 (1997).
[6] R. Heyd, A. Charlier, and E. McRae, Phys. Rev. B **55**, 6820 (1997).
[7] L. Yang, M. P. Anantram, J. Han, and J. P. Lu, Phys. Rev. B **60**, 13874 (1999).
[8] L. Yang and J. Han, Phys. Rev. Lett. **85**, 154 (2000).
[9] A. Kleiner and S. Eggert, Phys. Rev. B **63**, 073408 (2001).
[10] T. W. Tombler, C. W. Zhou, L. Alexseyev, J. Kong, H. J. Dai, L. Lei, C. S. Jayanthi, M. J. Tang, and S. Y. Wu, Nature (London) **405**, 769 (2000).
[11] A. Maiti, A. Svizhenko, and M. P. Anantram, Phys. Rev. Lett. **88**, 126805 (2002).
[12] J. Cao, Q. Wang, and H. J. Dai, Phys. Rev. Lett. **90**, 157601 (2003).
[13] E. D. Minot, Y. Yaish, V. Sazonova, J. Y. Park, M. Brink, and P. L. McEuen, Phys. Rev. Lett. **90**, 156401 (2003).
[14] W. P. Eaton and J. H. Smith, Smart Mater. Struct. **6**, 530 (1997).
[15] J. Kong, H. T. Soh, A. M. Cassell, C. F. Quate, and H. J. Dai, Nature (London) **395**, 878 (1998).
[16] H. T. Soh, C. F. Quate, A. F. Morpurgo, C. M. Marcus, J. Kong, and H. J. Dai, Appl. Phys. Lett. **75**, 627 (1999).
[17] A. Javey, J. Guo, Q. Wang, M. Lundstrom, and H. J. Dai, Nature (London) **424**, 654 (2003).
[18] D. Mann, A. Javey, J. Kong, Q. Wang, and H. J. Dai, Nano Lett. **3**, 1541 (2003).
[19] C. W. Zhou, J. Kong, and H. J. Dai, Phys. Rev. Lett. **84**, 5604 (2000).
[20] M. Ouyang, J. L. Huang, C. L. Cheung, and C. M. Lieber, Science **292**, 702 (2001).
[21] S. J. Tans, A. R. M. Verschueren, and C. Dekker, Nature (London) **393**, 49 (1998).
[22] J. W. Ding, X. H. Yan, and J. X. Cao, Phys. Rev. B **66**, 073401 (2002).
[23] P. E. Lammert, P. H. Zhang, and V. H. Crespi, Phys. Rev. Lett. **84**, 2453 (2000).
[24] T. Hertel, R. E. Walkup, and P. Avouris, Phys. Rev. B **58**, 13870 (1998).
[25] A. Maiti and A. Ricca, Chem. Phys. Lett. **395**, 7 (2004).
[26] Y.-K. Kwon and D. Tomanek, Phys. Rev. B **58**, R16001 (1998).
[27] S. Reich, C. Thomsen, and P. Ordejon, Phys. Rev. B **65**, 155411 (2002).
[28] G. T. A. Kovacs, *Micromachined Transducers Sourcebook* (McGraw-Hill, New York, 1998).
[29] C. L. Kane, E. J. Mele, R. S. Lee, J. E. Fischer, P. Petit, H. Dai, A. Thess, R. E. Smalley, A. R. M. Verschueren, S. J. Tans, and C. Dekker, Europhys. Lett. **41**, 683 (1998).

Downloaded 24 Feb 2005 to 171.64.120.244. Redistribution subject to AIP license or copyright, see http://apl.aip.org/apl/copyright.jsp